PNAS RESEARCH ARTICLE | BIOCHEMISTRY OPEN ACCESS

HDX-MS performed on BtuB in *E. coli* outer membranes delineates the luminal domain's allostery and unfolding upon B12 and TonB binding

Adam M. Zmyslowski[a], Michael C. Baxa[a], Isabelle A. Gagnon[a], and Tobin R. Sosnick[a,b,c,1]

Edited by Rachel Klevit, University of Washington, Seattle, WA; received October 23, 2021; accepted April 9, 2022

To import large metabolites across the outer membrane of gram-negative bacteria, TonB-dependent transporters (TBDTs) undergo significant conformational change. After substrate binding in BtuB, the *Escherichia coli* vitamin B12 TBDT, TonB binds and couples BtuB to the inner-membrane proton motive force that powers transport [N. Noinaj, M. Guillier, T. J. Barnard, S. K. Buchanan, *Annu. Rev. Microbiol.* 64, 43–60 (2010)]. However, the role of TonB in rearranging the plug domain of BtuB to form a putative pore remains enigmatic. Some studies focus on force-mediated unfolding [S. J. Hickman, R. E. M. Cooper, L. Bellucci, E. Paci, D. J. Brockwell, *Nat. Commun.* 8, 14804 (2017)], while others propose force-independent pore formation by TonB binding [T. D. Nilaweera, D. A. Nyenhuis, D. S. Cafiso, *eLife* 10, e68548 (2021)], leading to breakage of a salt bridge termed the "Ionic Lock." Our hydrogen–deuterium exchange/mass spectrometry (HDX-MS) measurements in *E. coli* outer membranes find that the region surrounding the Ionic Lock, far from the B12 site, is fully destabilized upon substrate binding. A comparison of the exchange between the B12-bound and the B12+TonB–bound complexes indicates that B12 binding is sufficient to unfold the Ionic Lock region, with the subsequent binding of a TonB fragment having much weaker effects. TonB binding accelerates exchange in the third substrate-binding loop, but pore formation does not obviously occur in this or any region. This study provides a detailed structural and energetic description of the early stages of B12 passage that provides support both for and against current models of the transport process.

mass spectrometry | hydrogen exchange | TonB-dependent transporters | allostery | outer membranes

Significance

TonB-dependent transporters such as BtuB are found in the outer membranes of gram-negative bacteria. They import scarce nutrients essential for growth, such as B12, the substrate of BtuB. Many transport steps remain enigmatic. Recent studies have emphasized force-mediated unfolding or the breakage of the "Ionic Lock," a moiety far from the B12 binding site. A strong dependence on the membrane environment has been noted. Accordingly, we measured hydrogen exchange on BtuB still embedded in native outer membranes and found that B12 binding is sufficient to break the Ionic Lock. The amino terminus then extends into the periplasm to bind TonB, but we find no evidence of pore formation, which likely requires energy transduction from the inner membrane by TonB.

TonB-dependent transporters (TBDTs) are ubiquitously found in the outer membranes (OMs) of gram-negative bacteria, where they import scarce nutrients (1). Some members of the family function as virulence factors, counteracting nutrient sequestration by the innate immune response (2). Aspects of the transport mechanism remain unclear, especially the nature of the structural changes involved in the creation of the pore required for substrate passage through the transmembrane β-barrel (3). Pore formation in each TBDT is tailored to its substrate, which can range in size from 56 Da (iron) to the 1.4-kDa cyanocobalamin (B12). In some TBDTs, the large extracellular loops close behind the substrate. This closure prevents back-diffusion (4), implying that formation of a pore through the lumen of the barrel need not imply bidirectional diffusion. Alternatively, the pore may form in stages, with no single conformation allowing for unrestricted diffusion across the length of the membrane. Though the individual mechanisms may be substrate-specific, pore formation generally involves conformational changes within the plug domain that normally occludes the lumen.

BtuB is a prototypical *Escherichia coli* TBDT that has been studied extensively in both functional and biophysical contexts (Fig. 1) (5–7). B12 is a relatively large TBDT substrate, which places constraints on the minimum pore size. In proposed models of pore formation (8, 9), B12 binding initiates an allosteric signaling event that leads to the release of the seven-residue, amino-terminal "Ton box" (10) into the periplasm, where it binds the periplasmic carboxyl-terminal domain (CTD) of TonB ($TonB_{CTD}$), an inner-membrane (IM) protein (11).

The steps leading from $TonB_{CTD}$–Ton box binding to the formation of a pore are currently under debate. The binding of $TonB_{CTD}$ enables the energetic, and possibly mechanical, coupling between the IM and OM that is necessary for transport against a B12 gradient (12). In the periplasm, TonB interacts with the ExbB–ExbD complex, which harvests the proton motive force of the IM (13). Though many structures of the TonB–ExbB–ExbD complex have recently been solved, the relationship between the transport mechanism and the assumed rotation of this IM complex on TBDTs remains

Author affiliations: [a]Department of Biochemistry and Molecular Biology, The University of Chicago, Chicago, IL 60637; [b]Prizker School for Molecular Engineering, The University of Chicago, Chicago, IL 60637; and [c]Institute for Biophysical Dynamics, The University of Chicago, Chicago, IL 60637

Author contributions: A.M.Z. and T.R.S. designed research; A.M.Z., M.C.B., and I.A.G. performed research; A.M.Z., M.C.B., and T.R.S. analyzed data; and A.M.Z., M.C.B., and T.R.S. wrote the paper.

The authors declare no competing interest.

This article is a PNAS Direct Submission.

[1]To whom correspondence may be addressed. Email: trsosnic@uchicago.edu.

This article contains supporting information online at http://www.pnas.org/lookup/suppl/doi:10.1073/pnas.2119436119/-/DCSupplemental.

Published May 12, 2022.

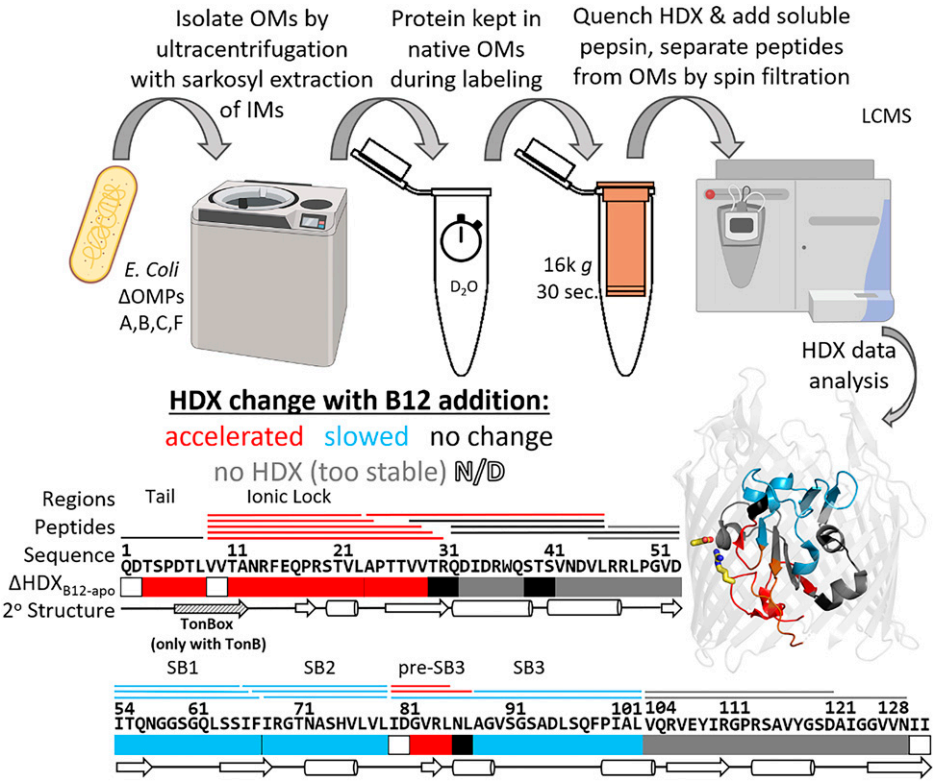

Fig. 1. BtuB purification and HDX protocol. Sample preparation in OMs involves no chromatography, only repeated centrifugation and resuspension with a sarkosyl extraction step to remove IMs. All steps except HDX labeling occur on ice. The structure shown is for the apo state of BtuB (PDB ID code 1NQE), with the β-barrel domain displayed transparently to highlight regions of the plug domain.

ambiguous (3). In force-dependent models, TonB transduces energy from the IM either by pulling the plug domain's amino terminus toward the periplasm (6, 8, 14) or by applying a torque (15). These forces are proposed to remodel the plug to form a pore, as seen in simulations (8, 16). Other steered molecular dynamics simulations have characterized the interactions of B12 as it is pulled through the lumen (17). Alternatively, pore formation has been proposed to be regulated in a force-independent manner by the Ionic Lock (IL), a conserved salt bridge between Arg14 on the plug and Asp316 on the nearby inner surface of the transmembrane β-barrel (9, 18). In the force-independent model, TonB binding need only disengage the IL to allow pore-forming motions in the third substrate-binding loop (SB3) when B12 is present (9).

In the B12-bound crystal structure of BtuB [Protein Data Bank (PDB) ID code 1NQH (7)], the IL region adopts a very similar backbone conformation to the apo state (PDB ID code 1NQE). The major change in the IL region is the rotation of the Arg14 side chain and the loss of the salt bridge with Asp316 (*SI Appendix*, Fig. S1). In the ternary complex with $TonB_{CTD}$, the IL is fully broken and the Arg14 C_α atom moves by 30.2 Å [PDB ID code 2GSK (6)]. This breakage occurs along with the residues immediately carboxyl-terminal to the Ton box adopting an extended conformation, which permits them to exit the lumen and bind $TonB_{CTD}$ (*SI Appendix*, Fig. S1).

Cafiso and coworkers have suggested that the folded IL region in B12-bound BtuB (PDB ID code 1NQH) is a feature resulting from crystallographic solutes and packing contacts perturbing the folding equilibrium (19). This potentially crucial difference leaves unresolved the actual conformation of the IL region in the B12-bound state in the native membrane. Determining when the IL region unfolds is important, as the subsequent binding of TonB has recently been proposed to be the critical event that breaks the IL rather than the binding of B12 (9). This ambiguity on how the amino-terminal region of BtuB responds to B12- and subsequent TonB-binding events is the focus of the present investigation.

Studying the forces that promote transport in the context of the intact cell envelope is desirable but so far has not been accomplished. Hence, most biophysical measurements of BtuB have been performed in reconstituted, single-bilayer systems. However, as recently emphasized (9), the results of these experiments have depended on the choice of environment, which have included detergents, liposomes, supported bilayers, OMs, or recently even live *E. coli* (20). The pore-forming intermediate state of BtuB has proven difficult to characterize, and efforts have relied on either extraction from native membranes, the use of cysteine mutants and spin labels, or a combination thereof (8, 20).

Here, we present a label-free investigation of the effects of B12 and $TonB_{CTD}$ binding on the conformation of the BtuB plug domain using hydrogen–deuterium exchange/mass spectrometry (HDX-MS) in OMs (Fig. 1). As anticipated, we find that the binding of B12 slows down HDX on the plug's three substrate-binding loops (Fig. 1, blue). Upon the binding of B12 alone, however, HDX is increased by 10^2- to 10^3-fold (i.e., destabilized) for at least a dozen residues surrounding the IL. These residues stretch from the carboxyl-terminal side of the Ton box to the beginning of the first β-strand (Fig. 1, red), supporting the proposal that a binding event breaks the IL as a prerequisite to transport (9). However, we find that the binding of B12 alone, rather than TonB, disrupts the IL. Accordingly, we propose that B12 binding leads to an allosterically induced unfolding of BtuB's amino terminus via breakage of the IL, which in turn enables TonB to bind the newly exposed Ton box (Fig. 1, red). In addition, we observe a mild acceleration

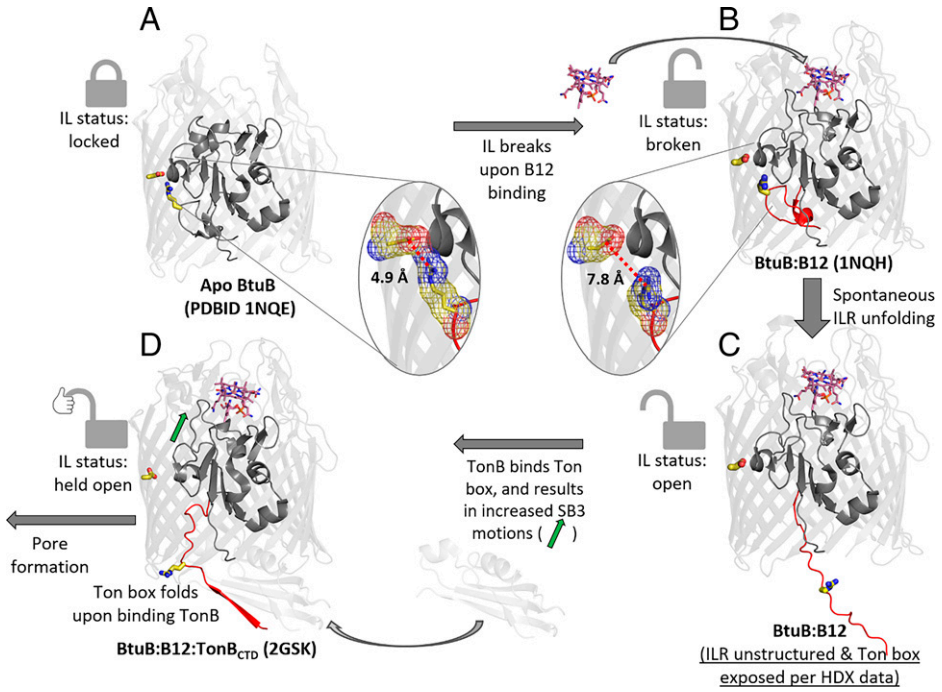

Fig. 2. Model of the BtuB plug domain's conformational response to two ligand-binding events. (*A*, *C*, and *D*) The three major steps identified by the HDX data. (*B*) A structure with bound B12 observed by crystallography but not observed in our data. The IL side chains are shown as yellow sticks, with oxygen and nitrogen atoms colored in red and blue, respectively. Ovals show an expanded mesh representation of the IL in states *A* and *B*. ILR, IL region.

within a four-residue segment located between the IL and the B12-contacting apex of the SB3 loop, which is near a site of pore formation recently proposed by Cafiso and coworkers (9). This colocalization suggests that B12 initiates only the first step in a cascade of events that promotes its own transport (Fig. 2). The binding of TonB is a subsequent step, but our results suggest that it too may be insufficient to cause pore formation in the absence of coupling to an active ExbB–ExbD complex. We end with a discussion of the similarity to prior findings (9) but also note some differences.

Results

We first discuss the protocols and reproducibility of our HDX measurements in OMs, followed by a presentation of the data for regions where stability increases due to B12 binding, focusing on the substrate-binding loops SB1 to SB3 (Fig. 3, shades of blue/green). We next describe the large decrease in stability observed near the IL and the smaller stability losses for regions at the nearby amino terminus, the first strand, and the start of the SB3 loop (Fig. 3, red shading). We conclude with an examination of the regions where minimal changes in HDX are seen upon B12 binding. To allow access to the HDX data of this study, we are including an HDX data summary (Table 1), HDX peptide summary (*SI Appendix*, Table S1), and HDX data tables (Dataset S1) (21).

OM Sample Preparation and Sequence Coverage. We measured deuterium uptake at pD 7.2 (pD_{read} = 6.8), 22 °C for apo and B12- and $TonB_{CTD}$-liganded states of BtuB labeled in native-like OMs from three biological replicates. To study the effects of $TonB_{CTD}$ binding, we used $TonB_{\Delta N}$, a construct containing the CTD and periplasmic linker but lacking the amino-terminal transmembrane helix (hereafter referred to as "TonB" within the context of our experiments). OMs and OM proteins (OMPs) are significantly more stable than their IM counterparts, and thus the protocols used to study OMPs employ strategies that are not as commonly used for IM proteins.

To our knowledge, the only published HDX-MS study of OMPs performed in a native OM-like environment was conducted on OmpF in *E. coli* OM vesicles (22). BtuB, however, did not express well in OM vesicles, so we adapted protocols used in electron paramagnetic resonance (EPR) studies of BtuB embedded in native-like OMs (23). Based on a purification strategy employed on FhuA (24), a BtuB construct was created with five histidines, one glycine, and two serines inserted after His449 on the apex of BtuB's seventh extracellular loop. This construct and the wild-type protein were overexpressed in *E. coli,* and, after lysis, total membranes were separated using ultracentrifugation followed by extraction with sarkosyl to selectively remove the IMs. Initially, the OMPs were extracted with detergent, but detergent-solubilized BtuB failed to exhibit evidence of B12 binding in the IL region by HDX, consistent with earlier findings that detergent solubilization perturbs the folding of the amino terminus (25). Hence, BtuB was left in its native OM environment for our HDX studies.

Accordingly, our workflow was altered to allow HDX labeling as well as digestion of BtuB still embedded in the OM preparations. After HDX labeling, we added denaturant and soluble pepsin in the low-pH quench buffer rather than employing an in-line protease column as typically done in HDX-MS measurements. This change in protocol afforded us greater control over the cleavage conditions while eliminating fouling of the chromatographic system by OM components such as lipids. We optimized digestion for redundant and nearly complete peptide coverage of the plug domain, in part by decreasing β-barrel cleavage (Fig. 1 and *SI Appendix*, Fig. S2*B*). Consistent with the known trends of BtuB unfolding in response to denaturant (26), the proteolysis was best near the amino terminus. Pepsin's weak preference to cleave after hydrophobic residues caused the peptides to cluster into regions with similar boundaries with peptides within each region exhibiting

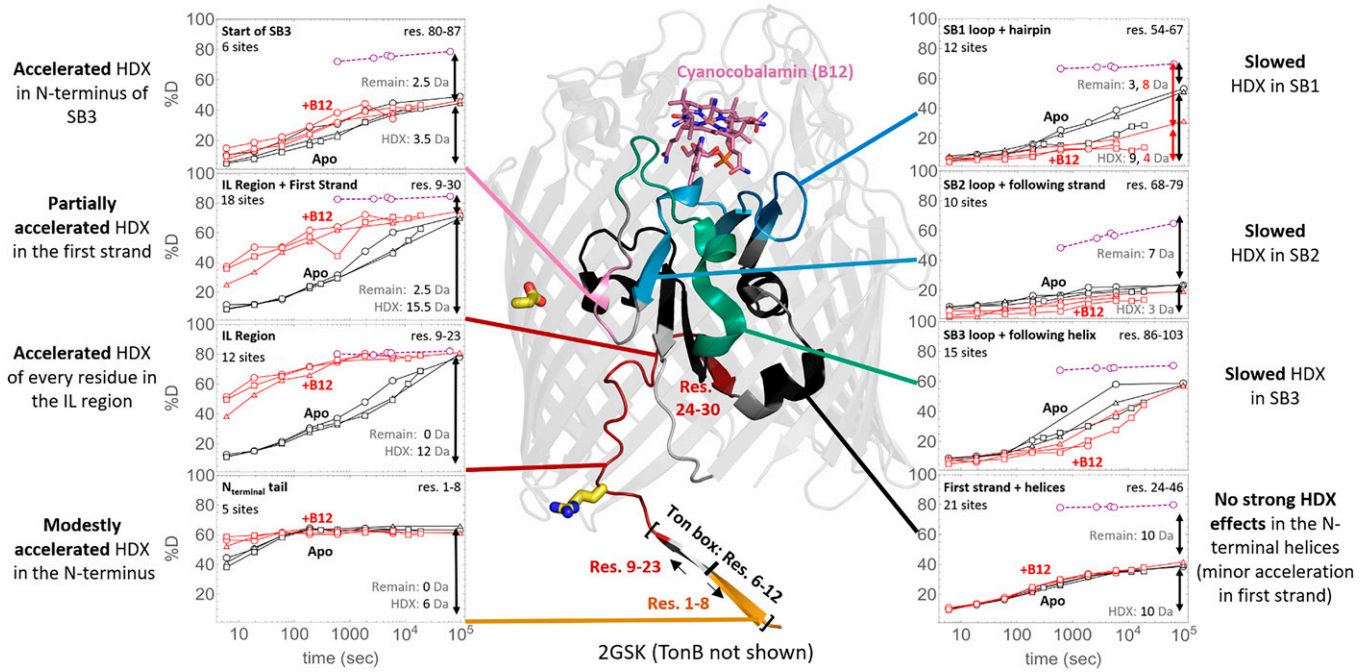

Fig. 3. Effects of B12 binding on HDX. Uptake plots show biologically triplicated data (circles, triangles, and squares) for BtuB measured in apo (black) and B12-bound (red) states. (*Insets*) Uptake curves for the peptides depicted by the colored regions on the BtuB structure. The number of exchangeable sites is assumed to be the number of nonproline residues minus 2. The exchanged and remaining masses at the last time point are given in gray, after correcting for back-exchange by normalizing to nonnative controls which are assumed to be fully deuterated (purple circles with dashed lines; for clarity, only five long time points are shown).

similar HDX behavior. We use a nomenclature where regions are capitalized while the sequence bounds are denoted in subscript, with important peptides in parentheses [e.g., BtuB's amino terminus is covered by $\text{Region}_{3–8}$ ($\text{Peptide}_{1–8}$)].

The imperfect correspondence between peptide and region boundaries is caused by an effect common to all HDX-MS studies. The intrinsic exchange rates for an exposed amide (k_{chem}) for the two amino-terminal residues are sufficiently fast that they largely lose their deuterium labels via back-exchange, and hence they do not measurably impact the deuterium uptake level (27). Consequently, we defined regions to start at the third residue of the most amino-terminal peptide of the cluster except for situations where other peptides can provide information for those residues. Our partitioning of the plug domain into regions typically coincided with the secondary-structure boundaries. Areas previously reported to undergo distinct motions usually separated into distinct regions (Fig. 3) (28). Despite each region having markedly different exchange behavior, peptides within a region were internally consistent with respect to their deuteration levels. Peptides spanning more than one region displayed intermediate effects, weighted by the number of amide protons in each region. While we have obtained peptide coverage sufficient to calculate site-resolved uptake at some positions, this is not generally possible. Accordingly, the analysis was conducted at the peptide level across the multiple replicates and conditions.

Reproducibility. Three biological replicates were initially prepared. One replicate used unmodified BL21 (DE3) *E. coli* whereas two replicates used a quadruple OMP knockout strain to examine the potential effects of endogenous OMPs (29). The use of the knockout strain did not significantly alter the HDX results (Figs. 3 and 4), although it did reduce the non-BtuB OMP content as desired (*SI Appendix*, Fig. S2*A*). One of the two knockout replicates had high levels of nonnative signals, complicating the analysis.

Our conclusions regarding B12 binding hold for every presented peptide across all replicates, though minor features of HDX uptake trends varied between biological replicates (Fig. 4). For the major population, the only significant difference between biological replicates is that one showed a diminished effect of $\text{TonB}_{\Delta N}$ binding (Fig. 4*B*). Optimization of integration bounds for our data resulted in the apo state's deuterium level having an SD of ∼0.36 Da when averaged across the 35 presented peptides. Dataset S1 provides estimates of mass differences significant at the 98% confidence level for each peptide. These intervals varied from 0.33 ($\text{Peptide}_{1–8}$) to 7.31 Da ($\text{Peptide}_{80–103}$) and had a mean of 1.75 Da and median of 1.39 Da. The average level of back-exchange observed in our data was 25%, with an interquartile range of 9.0%. Further plots summarizing the reproducibility are provided in *SI Appendix*, Fig. S3 and Table S1.

Substrate-Binding Loops. In apo BtuB, substrate-binding loops SB1 to SB3 exchanged slowly, with most associated peptides retaining greater than 50% of their H level even after 10^5 s, the longest measured time point. This slow exchange translates to an HDX protection factor (PF) $>10^5$, where PF is defined as the relative slowing of the observed HDX rate (k_{obs}) compared with k_{chem}: $\text{PF} = k_{\text{chem}}/k_{\text{obs}}$ (see *SI Appendix* for HDX formalism and inference of EX2 behavior). Exchange was further slowed in the presence of 20 μM B12. An examination of overlapping peptides indicated that this slowing was concentrated in the residues nearer to the B12 binding site. Sites in SB1 had the largest decrease in fractional deuterium uptake, followed by SB2 and SB3 (*SI Appendix*, Fig. S4). In the presence of B12, the exchange rates for the few observable sites on SB2 were about 10-fold slower, although most sites already exchanged very slowly in the apo state, making any changes difficult to

Table 1. Biochemical and statistical details for each measured state

Dataset	Apo BtuB	BtuB + B12	BtuB + TonB	BtuB + B12 + TonB (ternary)
HDX reaction details	46.7 mM Na_2HPO_4, 0.6 mM Tris, pD_{read} = 6.80, 22 °C	46.7 mM Na_2HPO_4, 0.6 mM Tris, pD_{read} = 6.80, 20 μM B12, 1 mM $CaCl_2$, 22 °C	46.7 mM Na_2HPO_4, 0.6 mM Tris, pD_{read} = 6.80, 22 °C	46.7 mM Na_2HPO_4, 0.6 mM Tris, pD_{read} = 6.80, 2 μM B12, 1 mM $CaCl_2$, 22 °C
HDX time course, min	0.1, 0.316, 1.0, 3.16, 10, 31.6, 100, 316, 1,620	0.1, 0.316, 1.0, 3.16, 10, 31.6, 100, 316, 1,620	0.1, 0.33, 1.0, 3.5, 10, 36	0.1, 0.316, 1.0, 3.16, 10, 31.6, 100, 316
HDX control samples	Maximally labeled control (LH4 construct, His-tagged on extracellular loop)	Maximally labeled control (LH4 construct, His-tagged on extracellular loop)	Maximally labeled control (LH4 construct, His-tagged on extracellular loop)	Maximally labeled control (LH4 construct, His-tagged on extracellular loop)
Back-exchange, mean/IQR	25.1%/8.5%	25.1%/8.5%	25.2%/9.3%	25.0%/8.8%
No. of peptides	35	35	29	31
Sequence coverage	95.4% (of 130 residues covering N terminus and plug domain) 21.2% (whole protein)	95.4% (of 130 residues covering N terminus and plug domain) 21.2% (whole protein)	90% (of 130 residues covering N terminus and plug domain) 19.7% (whole protein)	90% (of 130 residues covering N terminus and plug domain) 19.7% (whole protein)
Average peptide length/redundancy	16.5/0.7	16.5/0.7	16.5/0.7	15.9/0.6
Replicates	3 (biological)	3 (biological)	1	3 (biological)
Repeatability	3.24%/0.36 Da (average SD)	2.93%/0.34 Da (average SD)	N/A	6.42%/0.86 Da (average SD)
Significant differences in HDX (ΔHDX > X Da)	1.75 Da (98% CI)	1.62 Da (98% CI)	N/A	4.15 Da (98% CI)

IQR, interquartile range; N/A, not applicable.

discern (*SI Appendix*, Fig. S4.15–24). Whereas the overall exchange for SB3 was slowed only 5-fold, some peptides displayed complex behavior, and exchange for other peptides was even accelerated, as will be discussed later. Otherwise, the general slowing of HDX upon the addition of B12 in the three substrate-binding loops indicates that B12 binding stabilizes regions directly contacting the substrate.

Allosteric Destabilization of the IL and Ton Box upon B12 Binding. Our major finding is that upon B12 binding, exchange drastically increased for the IL $Region_{11–23}$ ($Peptides_{9–23}$, $_{9–27}$, $_{9–28}$, $_{9–29}$, and $_{9–30}$). The IL region contains the Arg14–Asp316 salt bridge that connects the plug domain to the inner wall of the β-barrel (Fig. 4 and *SI Appendix*, Fig. S4.2–6). In addition, exchange was mildly increased for the amino-terminal tail $Region_{3–8}$ (*SI Appendix*, Fig. S4.1). Peptides in the IL region exchanged up to 10^3-fold faster with B12, with a majority of the exchange occurring within the 6-s dead time of the measurement. For the tail region, deuterium uptake increased mildly, with the uptake increasing from 50 to 80% after 6 s. From this widespread acceleration of HDX, we infer that both regions are unfolded in the B12-bound state and that upon B12 binding the amino terminus partially exits the lumen. The smaller change in HDX for the tail region is the result of it being less stable in the apo state to begin with.

We interpret the sizable B12 effect on the HDX of the IL region to result from the breaking of interactions between residues within this region and the β-barrel, most importantly the Arg14–Asp316 salt bridge. This disruption results in the Ton box's exit into the periplasm. Residues 1, 2, 9, and 10 are the first two residues on each of their respective peptides and thus unobservable due to back-exchange (an inherent HDX-MS issue occurring during sample handling). These four residues likely are also unstructured given the rapid exchange of every observable residue surrounding them (e.g., $Peptides_{1–8}$ and $_{9–23}$). Notwithstanding, the data provide strong evidence that BtuB's first 23

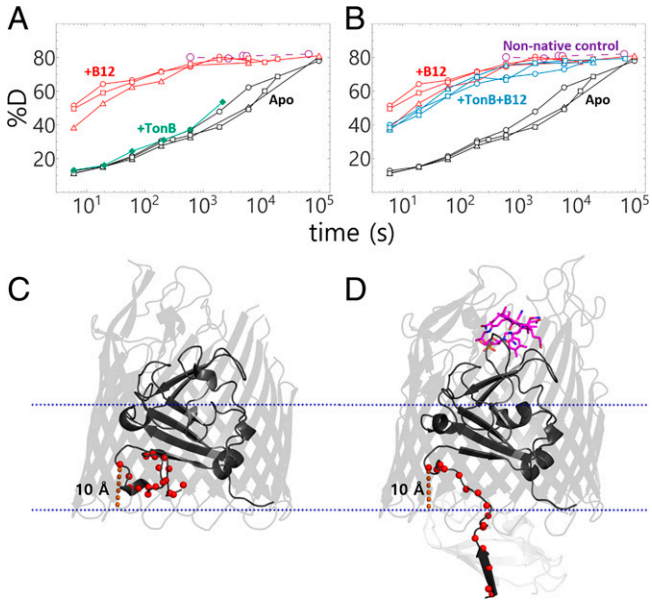

Fig. 4. HDX in the IL region. (*A* and *B*) Uptake plots for $Peptide_{9–23}$, with three biological replicates: apo (black), B12 (red), and $TonB_{ΔN}$ (green). Five long points of a nonnative control are shown in purple. (*B*) Uptake plots for $Peptide_{9–23}$, apo (black), B12 (red), and B12 + $TonB_{ΔN}$ (blue) (*C* and *D*): position of the amino-terminal regions relative to the membrane plane. (*C* and *D*) Apo (PDB ID code 1NQE) (*C*) and BtuB–B12–TonB complex (PDB ID code 2GSK) (*D*) crystal structures, taken from the OPM database (32). N atoms for residues 6 to 23 are shown as red spheres. Distances from Leu23's N atom to the nearest membrane-plane dummy atom are shown as dashed orange lines, in both cases about 10 Å.

residues undergo a complete or near-complete loss of structure in response to B12 binding. One might suppose the opposite situation, where a sizable population of folded IL remains after B12 addition but exchanges via localized fluctuations for residues not encompassing the entire IL region; however, this scenario should, upon the addition of TonB, shift the equilibrium to an increased unfolded IL population and a corresponding acceleration of HDX for at least part of the IL region. The opposite, however, was observed, suggesting that the IL was broken for a majority of BtuB molecules in the presence of B12 alone.

Our inference that both the IL region and the Ton box were unfolded upon B12 binding alone is further supported by our finding that the addition of $TonB_{\Delta N}$ did not further accelerate exchange. The binding of TonB (specifically the carboxyl-terminal domain) to the Ton box requires that the Ton box be extended into the periplasm, which in turn requires that the IL be broken. Therefore, if the IL region remained folded after B12 binding and then unfolded when $TonB_{\Delta N}$-bound, one would have expected a marked increase in exchange for the IL region upon $TonB_{\Delta N}$ binding. However, exchange did not markedly increase upon the addition of $TonB_{\Delta N}$ (in fact, exchange even slowed for a few residues, which provides direct evidence of TonB binding) (*SI Appendix*, Fig. S4.2–6). This minimal increase in exchange is in the opposite direction of what would be expected if B12 binding did not cause the IL to break. Therefore, the IL region is already unfolded prior to $TonB_{\Delta N}$ binding, and B12 binding alone is sufficient to unfold the IL region.

In ostensible disagreement with this conclusion is that the IL region retains a significant amount of HDX protection even after B12 binding. The deuterium buildup curve is $\sim 10^2$-fold slower than what would be expected for exposed amides in bulk solution (27). To rationalize the observed slowing, we propose that the bulk solution rate may be an inappropriate reference in the present situation as the IL region's carboxyl terminus is located 10 Å inside the barrel lumen, which prevents portions of the region from fully exiting into bulk solvent. In this partially confined state inside the barrel, the access of OD^- to the peptide backbone also could be reduced and exchange slowed. The residues that do exit into the periplasm may still be subject to a milder but similar blocking effect from interactions with the nearby peptidoglycan (*SI Appendix*, Fig. S5). In addition, the effective $[OD^-]$ should be lower in the barrel than in the bulk solvent, as the anion prefers to be hydrated rather than reside in the lumen's lower dielectric environment (30). Both the reduced access to the backbone and lower $[OD^-]$ concentration would retard exchange and may account for the slower than expected exchange observed upon B12 binding for the IL and for other regions, especially those further inside the barrel.

In the B12-bound state, Cafiso and coworkers proposed that the IL is broken and were able to infer residues 1 to 15 as being unstructured (10). Early EPR measurements probing the Ton box found that B12 binding caused the first residue within the Ton box, Asp6, to project 20 to 30 Å into the periplasm, leading the authors to model the first 15 residues as exiting the lumen with a broken IL (10). Consistently, our HDX-MS measurements also identified this sizable unstructured region, finding that it extends out to residue 23. We observed rapid deuteration of every observable amide out to residue 23 ($Peptides_{1–8}$ and $_{9–23}$), suggesting that an additional eight residues are affected by the same B12-binding event. Hence, we have evidence of a B12-initiated unfolding that is larger than previously described.

A comparison of $Peptide_{9–23}$ with the overlapping $Peptides_{9–27}$, $_{9–28}$, $_{9–29}$, and $_{9–30}$ indicates that acceleration of HDX was also occurring in some additional residues between 24 and 29, which encompass BtuB's first β-strand (*SI Appendix*, Fig. S4.7–12). This acceleration did not equally affect all five exchangeable residues, however. The exchange for some residues within BtuB's first β-strand remained very slow, implying that the strand remains folded with its outer edge becoming more solvent-exposed when B12 binds. In sum, we have used HDX to quantify the size of the B12-mediated unfolding in BtuB's amino terminus.

Complex Ligand Effects in the Third Substrate-Binding Loop, Including Destabilization by B12. In sharp contrast to the generally slowed exchange observed for the substrate-binding loops, the amino terminus of SB3 ($Region_{82–85}$) exhibited accelerated exchange upon B12 binding (*SI Appendix*, Fig. S4.24). The apparent timescale of exchange for the fastest amide proton among residues 82 to 85 on $Peptide_{80–85}$ was ∼2,000 s, with B12 binding resulting in a faster exchange rate of this single amide by ∼5-fold. Other amides within $Region_{82–85}$ remained too protected to be observed exchanging in our experiments, so the data are agnostic on whether these positions were affected by B12, unlike the remaining portion of SB3 ($Region_{86–103}$) and the other SBs, which were affected (*SI Appendix*, Fig. S4. 15–23). The change in HDX for $Region_{82–85}$ upon B12 binding was relatively mild compared with that seen at the amino terminus of the protein. This region, however, was unique in having its exchange further enhanced beyond the already B12-accelerated rates by the addition of $TonB_{\Delta N}$ (*SI Appendix*, Fig. S4.24). Hence, the SB3 region allosterically responds to distal binding of B12 as well as TonB-binding events, supporting its relevance to the TonB-dependent transport mechanism (9). Two reasons may explain the relatively small changes in HDX observed in the SB3 region. Possibly, one end of the SB3 loop is accelerated while the other end is slowed by binding B12, yielding a small net change in uptake. Additionally, rather than pore formation, the small changes may reflect a modest change in H bonding across the region.

Regions with No Significant HDX Differences. The HDX of the three remaining regions of the plug domain did not display a significant response to B12 binding (*SI Appendix*, Fig. S4. 11–13 and S4.33–35). Two of these regions ($Regions_{30–46}$ and $_{47–53}$) lie between the IL and SB1 while the third region ($Region_{104–128}$) is carboxyl-terminal to SB3. A comparison of overlapping peptides within $Region_{30–46}$ (*SI Appendix*, Fig. S4. 11 and S4.12) confirmed the mild response to B12 within residues 26 to 29, as discussed earlier, demonstrating that the residues flanking BtuB's first stable helix do not respond to B12. $Regions_{47–53}$ and $_{104–128}$ (*SI Appendix*, Fig. S4.33–35) exhibited almost no exchange, being extremely stable. The high overall stability for these regions and apparent lack of a response to ligand binding suggest that rearrangements in the plug domain during ligand binding are restricted to the areas surrounding the IL and SB3. Strictly speaking, however, we must be agnostic on potential changes for residues that exchange outside our experimental time window.

Discussion

Our major observation is that the binding of B12 promotes the complete breaking of the IL (30), a critical salt bridge connecting the amino-terminal end of the plug domain to the inner surface of the β-barrel (Arg14–Asp316). The breakage results in all of the residues within $Region_{11–23}$ unfolding, exposing the Ton box and permitting TonB binding. Upon subsequent

TonB binding to the B12-bound state, we did not observe evidence of pore formation or further unfolding of the IL region. In fact, TonB binding alone only produced subtle HDX changes throughout the plug domain, suggesting that its full function in pore formation requires an energized IM, or some other factor only present in live cells.

Binding of B12 alone resulted in stability changes throughout the plug domain, both increasing and decreasing HDX rates. We observed the anticipated slowing of exchange for the loops that directly contact B12. But the addition of B12 also resulted in a dramatic acceleration of HDX by up to 10^3-fold for all amide protons in the IL region (e.g., $Peptide_{9–23}$), even approaching the rapid exchange rates seen in BtuB's labile amino terminus ($Peptide_{1–8}$). The large increase in HDX rates upon B12 binding for residues in the Ton box reflects the disruption of the entire IL region (residues 11–23) and can occur in response to B12 binding alone. We believe this disruption is responsible for exposing the Ton box, thereby regulating TonB binding.

The IL is over 20 Å away from the B12 binding site, implying an allosteric mechanism is involved in the breaking of this salt bridge. The amino-terminal segment of SB3, $Region_{82–85}$, is located near the IL and is also accelerated by B12 binding, pointing to the involvement of SB3 in the allosteric mechanism. Additionally, HDX of $Region_{82–85}$ is further accelerated by the binding of TonB to the Ton box, suggesting a bidirectional coupling of one or both Ton box–containing regions with the SB3 loop. The movement of SB3 upon B12 binding likely is a critical initial step in the signal propagation downward to the IL. Overall, our data support Cafiso and coworkers' proposal that SB3 may undergo further motions upon TonB binding (9).

As discussed earlier, even with a 10^2- to 10^3-fold increase in exchange rate for the IL $Region_{11–23}$ upon binding B12, HDX is still 10^2-fold slower than the intrinsic exchange rate k_{chem}. One might consider that this residual protection is indicative of some apparent structure in the IL region. However, evidence exists that this region is indeed unfolded: Because the binding of $TonB_{\Delta N}$ resulted in no further unfolding of the IL region after B12 binding, the IL must already have been broken and the region unfolded in the B12-bound state. Therefore, we propose that the 10^2-fold residual protection arises from other factors including restricted access to the peptide backbone, as the region is tethered inside the lumen, as well as a reduction of the local [OD^-] in the lumen's lower dielectric environment (30). Additionally, H-bonding interactions with the peptidoglycan network, which normally undergird the inner surface of the OM, may be conferring protection even to an otherwise unstructured chain. Further studies are needed to examine which, if any, of the three mechanisms is operational.

Comparisons with Existing Models. Current models of BtuB transport can be broadly separated into two categories based on the proposed location and energetics of pore formation, including whether it is force-independent (FI) or force-dependent (FD). In both models, either implicitly or explicitly, the binding of B12 is necessary for exposure of the Ton box and subsequent TonB binding. In the FI model (9), TonB binding provides the energy for subsequent plug remodeling events, which are sufficient to open a pore near the IL region and permit B12 transport. By contrast, a recent FD model proposes that TonB binding establishes a mechanical linkage that transmits a force to unfold the "mechanically weak subdomain" within the plug (8). This partial unfolding of the plug forms a substrate channel, although some uncertainty exists regarding whether this mechanism applies in vivo (9).

While the results of our experiments do not fundamentally rule out either model, our HDX data demonstrate that binding of B12 alone is sufficient to disrupt the IL region and expose the Ton box. However, our data find that neither the individual B12- nor TonB-binding events are sufficient to destabilize a substantial fraction of the plug domain, which is postulated to unfold under the FD model ($Regions_{31–46}$, $_{47–53}$, and $_{54–67}$). Peptides in $Region_{45–53}$ did not exchange in the duration of our measurements (10^5 s), implying a very high stability ($Peptide_{45–53}$; PF > 10^7). Flanking regions that unfold in the FD model [as observed in an atomic force microscopy study (8)] were either unaffected ($Peptide_{31–46}$; PF ~10^4) or even stabilized ($Peptide_{54–67}$; PF ~10^3 to 10^6) upon B12 binding. We believe that this high level of stability is unlikely, but not impossible, within the FD model (8). Our data also corroborate the argument (9) deployed against FD models related to the application of a torque on BtuB by TonB (15). We found that in the ternary complex of BtuB, B12, and TonB, nearly a dozen residues between the Ton box and BtuB's stably folded core are unstructured, consistent with findings for FhuA (31). For these residues, the facile rotation of their (ϕ,ψ) backbone torsion angles likely precludes the transmission of a torque directly from the Ton box to the plug.

Nevertheless, our HDX results also differ with the FI model regarding the effects of ligand binding. We find that the IL is broken by B12 binding alone, whereas Cafiso and coworkers (9) found in vivo that the IL is partially broken by B12 and only completely broken by TonB, based on the conformational response of the SB3 loop to B12 binding. Specifically, mutations that broke the IL (Arg14Ala, Asp316Ala) resulted in a 20-Å movement in SB3 and were reported to mimic TonB binding. In OMs, however, we find that the IL fully breaks in response to B12 binding and, additionally, that the IL is not broken by TonB binding at a concentration of 26 μM when B12 is absent. When B12 is added, however, we find the IL is sufficiently destabilized that subsequent TonB binding does not cause a significant slowing or acceleration of the HDX for the IL region. In our view, the Ton box is normally sequestered in the lumen of the β-barrel and becomes available for binding only when B12 binding allosterically induces the breakage of the IL. In this mechanism, the rest of the steps required to gate the pore are unlikely to begin before the initial B12-binding event.

Whereas Cafiso and coworkers (9) observed a 20-Å conformational change in SB3, we detected subtle HDX changes for this region upon B12 and TonB binding (*SI Appendix*, Fig. S4.24 and S4.25). It is difficult to reconcile large-scale motions occurring in SB3 with the lack of a large HDX effect for peptides covering the apex of SB3, especially since a 10^3-fold increase was seen in the IL region. Possible explanations for the difference include our use of sarkosyl to remove IMs (9) and the EPR study's use of live cells, which differs from our OM preparation. Furthermore, the two techniques measure very different quantities and timescales from which protein motions are inferred. HDX is sensitive to H bonding whereas EPR provides distance information from the static dipolar interaction between spin probes.

In our HDX-MS measurements, the introduction of TonB and formation of the ternary complex reduced the signal quality for certain peptides due to chromatographic overlap and mass spectral crowding. For certain SB3 peptides, deuterium uptake trends were complex even with B12 alone. Further study of this behavior may shed additional light on the allosteric mechanism.

Conclusions

Using HDX-MS, we identified regions of the BtuB plug domain that both increase and decrease stability upon substrate binding. Most notably, the binding of B12 alone is sufficient to initiate an allosteric pathway involving the disruption of a dozen residues located up to 20 Å away from the B12 binding site. The process involves the unfolding of the IL region to permit the binding of TonB to the Ton box.

The remaining steps in the transport process are less clear. Potentially, an exit channel forms that follows a route from the B12 binding site, past SB3, and then out through the space formerly occupied by the IL region. Alternatively, TonB binding may initiate the force-induced unfolding of the plug core to create a substrate channel. This latter mechanism is appealing in its simplicity and generalizability, as one can envision the role of substrate binding is simply to release the Ton box into solution where forces are applied by TonB, and the channel is then formed by the unfolding of approximately half of the plug domain core. However, the HDX data indicate that the core of the plug remains extremely stable when B12 and TonB are bound, providing a powerful example of how HDX's ability to access local thermodynamic information can help identify mechanisms. Besides the study of mutations that constitutively break the IL or disrupt potential allosteric pathways that cross the membrane, the measurement of the denaturant dependence of the HDX (27) could further define the conformational changes resulting from binding and force.

Because results across multiple techniques have depended on the membrane environment, future BtuB studies should be performed in as native-like a context as possible (9). Our application of HDX-MS in native OMs is a compromise between working in live cells, where transport intermediates may not accumulate due to the action of TonB, and reconstituted systems such as detergents (which do not bind B12) or liposomes (which are compositionally very different from OMs). The use of OMs provides both a native-like bilayer and high yield, which may enable the ambitious goal of performing HDX in vivo.

Materials and Methods

OMs used for HDX experiments were obtained by French press lysis of *E. coli* overexpressing BtuB followed by several rounds of centrifugation and a brief extraction with sarkosyl to selectively remove IMs. HDX labeling was initiated by diluting concentrated suspensions of the OMs into deuterated solutions. HDX labeling was terminated and digestion was simultaneously initiated by diluting the HDX labeling reaction into ice-cold quench buffer (pH 2.5) previously supplemented with urea, soluble pepsin, microporous zirconium oxide beads, and n-Dodecyl-B-D-Maltoside (DDM). After a brief incubation period, the labeled peptides released into solution were separated from insoluble undigested protein and membranes by spin filtration immediately before injection onto the liquid chromatography-mass spectrometry system. Further details are described in *SI Appendix, Materials and Methods*.

Chemicals were purchased from Sigma-Aldrich unless otherwise noted in *SI Appendix, Materials and Methods*. All BtuB and TonB constructs were expressed and purified as described in *SI Appendix, Materials and Methods*.

Data Availability. HDX update analysis data are included in the article and/or supporting information. Other data are available upon request.

ACKNOWLEDGMENTS. We thank R. Nakamoto, H. Hong, N. Noinaj, E. Perozo, M. Clark, and members of the T.R.S. laboratory for valuable conversations about TBDT biology, comments on the manuscript, or for kindly supplying plasmids and cell strains.

1. K. Schauer, D. A. Rodionov, H. de Reuse, New substrates for TonB-dependent transport: Do we only see the 'tip of the iceberg'? *Trends Biochem. Sci.* **33**, 330–338 (2008).
2. M. Miethke, M. A. Marahiel, Siderophore-based iron acquisition and pathogen control. *Microbiol. Mol. Biol. Rev.* **71**, 413–451 (2007).
3. H. Celia, N. Noinaj, S. K. Buchanan, Structure and stoichiometry of the Ton molecular motor. *Int. J. Mol. Sci.* **21**, 375 (2020).
4. C. R. Smallwood *et al.*, Concerted loop motion triggers induced fit of FepA to ferric enterobactin. *J. Gen. Physiol.* **144**, 71–80 (2014).
5. N. Noinaj, M. Guillier, T. J. Barnard, S. K. Buchanan, TonB-dependent transporters: Regulation, structure, and function. *Annu. Rev. Microbiol.* **64**, 43–60 (2010).
6. D. D. Shultis, M. D. Purdy, C. N. Banchs, M. C. Wiener, Outer membrane active transport: Structure of the BtuB:TonB complex. *Science* **312**, 1396–1399 (2006).
7. D. P. Chimento, A. K. Mohanty, R. J. Kadner, M. C. Wiener, Substrate-induced transmembrane signaling in the cobalamin transporter BtuB. *Nat. Struct. Biol.* **10**, 394–401 (2003).
8. S. J. Hickman, R. E. M. Cooper, L. Bellucci, E. Paci, D. J. Brockwell, Gating of TonB-dependent transporters by substrate-specific forced remodelling. *Nat. Commun.* **8**, 14804 (2017).
9. T. D. Nilaweera, D. A. Nyenhuis, D. S. Cafiso, Structural intermediates observed only in intact *Escherichia coli* indicate a mechanism for TonB-dependent transport. *eLife* **10**, e68548 (2021).
10. Q. Xu, J. F. Ellena, M. Kim, D. S. Cafiso, Substrate-dependent unfolding of the energy coupling motif of a membrane transport protein determined by double electron-electron resonance. *Biochemistry* **45**, 10847–10854 (2006).
11. D. M. Freed, S. M. Lukasik, A. Sikora, A. Mokdad, D. S. Cafiso, Monomeric TonB and the Ton box are required for the formation of a high-affinity transporter-TonB complex. *Biochemistry* **52**, 2638–2648 (2013).
12. N. Cadieux, R. J. Kadner, Site-directed disulfide bonding reveals an interaction site between energy-coupling protein TonB and BtuB, the outer membrane cobalamin transporter. *Proc. Natl. Acad. Sci. U.S.A.* **96**, 10673–10678 (1999).
13. A. A. Ollis, K. Postle, Identification of functionally important TonB-ExbD periplasmic domain interactions in vivo. *J. Bacteriol.* **194**, 3078–3087 (2012).
14. D. P. Chimento, R. J. Kadner, M. C. Wiener, Comparative structural analysis of TonB-dependent outer membrane transporters: Implications for the transport cycle. *Proteins* **59**, 240–251 (2005).
15. P. E. Klebba, ROSET model of TonB action in gram-negative bacterial iron acquisition. *J. Bacteriol.* **198**, 1013–1021 (2016).
16. J. Gumbart, M. C. Wiener, E. Tajkhorshid, Mechanics of force propagation in TonB-dependent outer membrane transport. *Biophys. J.* **93**, 496–504 (2007).
17. T. Pieńko, J. Trylska, Extracellular loops of BtuB facilitate transport of vitamin B12 through the outer membrane of *E. coli*. *PLoS Comput. Biol.* **16**, e1008024 (2020).
18. S. M. Lukasik, K. W. Ho, D. S. Cafiso, Molecular basis for substrate-dependent transmembrane signaling in an outer-membrane transporter. *J. Mol. Biol.* **370**, 807–811 (2007).
19. D. M. Freed, P. S. Horanyi, M. C. Wiener, D. S. Cafiso, Conformational exchange in a membrane transport protein is altered in protein crystals. *Biophys. J.* **99**, 1604–1610 (2010).
20. D. A. Nyenhuis, T. D. Nilaweera, D. S. Cafiso, Native cell environment constrains loop structure in the *Escherichia coli* cobalamin transporter BtuB. *Biophys. J.* **119**, 1550–1557 (2020).
21. G. R. Masson *et al.*, Recommendations for performing, interpreting and reporting hydrogen deuterium exchange mass spectrometry (HDX-MS) experiments. *Nat. Methods* **16**, 595–602 (2019).
22. D. Donnarumma *et al.*, Native state organization of outer membrane porins unraveled by HDx-MS. *J. Proteome Res.* **17**, 1794–1800 (2018).
23. A. Sikora, B. Joseph, M. Matson, J. R. Staley, D. S. Cafiso, Allosteric signaling is bidirectional in an outer-membrane transport protein. *Biophys. J.* **111**, 1908–1918 (2016).
24. G. S. Moeck *et al.*, Ligand-induced conformational change in the ferrichrome-iron receptor of *Escherichia coli* K-12. *Mol. Microbiol.* **22**, 459–471 (1996).
25. G. E. Fanucci, N. Cadieux, R. J. Kadner, D. S. Cafiso, Competing ligands stabilize alternate conformations of the energy coupling motif of a TonB-dependent outer membrane transporter. *Proc. Natl. Acad. Sci. U.S.A.* **100**, 11382–11387 (2003).
26. R. H. Flores Jiménez, D. S. Cafiso, The N-terminal domain of a TonB-dependent transporter undergoes a reversible stepwise denaturation. *Biochemistry* **51**, 3642–3650 (2012).
27. Y. Bai, J. S. Milne, L. Mayne, S. W. Englander, Primary structure effects on peptide group hydrogen exchange. *Proteins* **17**, 75–86 (1993).
28. C. Balusek, J. C. Gumbart, Role of the native outer-membrane environment on the transporter BtuB. *Biophys. J.* **111**, 1409–1417 (2016).
29. I. Meuskens, M. Michalik, N. Chauhan, D. Linke, J. C. Leo, A new strain collection for improved expression of outer membrane proteins. *Front. Cell. Infect. Microbiol.* **7**, 464 (2017).
30. H. Gong, G. Hocky, K. F. Freed, Influence of nonlinear electrostatics on transfer energies between liquid phases: Charge burial is far less expensive than Born model. *Proc. Natl. Acad. Sci. U.S.A.* **105**, 11146–11151 (2008).
31. J. L. Sarver, M. Zhang, L. Liu, D. Nyenhuis, D. S. Cafiso, A dynamic protein-protein coupling between the TonB-dependent transporter FhuA and TonB. *Biochemistry* **57**, 1045–1053 (2018).
32. M. A. Lomize, I. D. Pogozheva, H. Joo, H. I. Mosberg, A. L. Lomize, OPM database and PPM web server: Resources for positioning of proteins in membranes. *Nucleic Acids Res.* **40**, D370–D376 (2012).